RE-EVALUATION OF SARMA'S METHOD
IN SLOPE STABILITY ANALYSIS

M.R. Selamat[1]

ABSTRACT

Sarma's procedure may not have been used as often as common methods of slices in the stability analyses of static earth slopes. However, as the effects of ground vibration are increasingly taken into account in the stability analyses of many slopes, the suitability of Sarma's method for such applications is undoubtedly agreed by most engineers. In this study, a complete derivation of Sarma's analysis is re-evaluated. It also includes Hoek's modification (Hoek, 1987) of the original Sarma's formulation (Sarma, 1973, 1975, 1979; and Sarma and Bhave, 1974) to which a minor rectification is made. The associated important features of the method namely: Factor of Safety (FOS) versus acceleration curve, static FOS, and critical acceleration are highlighted. The FOS-acceleration curve shows that Sarma's method is capable of analyzing static as well as dynamic slope stability problems. Static FOS is FOS at zero acceleration while critical acceleration or ground acceleration at the threshold of failure is the acceleration when FOS equals unity. The fact that FOS-acceleration curves of different slopes can occupy different positions relative to FOS-acceleration axes and that ground can easily be moved by sources such as earthquake, production blasts in mines, traffic, pile driving and other construction activities, demolition blast, and nuclear detonation; it is proposed that it is necessary to present both, static FOS and critical acceleration, as indicators of stability for all slopes. By means of an actual case study, it is demonstrated that the extended Sarma method provides the essential results for a more complete assessment of slope stability.

INTRODUCTION

In practice, there are many instances where slopes designed for static loading are actually subjected to dynamic loads due to ground movements. Ground vibrations can originate from common day-to-day sources such as traffic, heavy equipment operation, and construction activities. Earthquakes, production blasts in mines, and detonations of various purposes also create ground excitations of considerable magnitude. Basically, it is difficult to imagine a slope which is free from the effects of one or another form of ground acceleration during its lifetime.

In Perak, Malaysia, in relation to this discussion, slopes of immediate interest are found in rock cuttings along the new North-South highway, on faces of limestone hills in Kinta Valley, and in quarries that are scattered throughout the state. Various instabilities at these slopes in the past might have been exacerbated by the presence of ground vibrations as recent failures have actually occurred within close proximity of heavy traffic or quarry activities (Selamat, 1996; and Selamat and Mohammad, 1996). Elsewhere in the world, engineers are becoming aware of the problems associated with slope stability especially in open pit mines where slopes are made larger for more profitable operation. For example, in a Western Australian mine, a major failure which was suspected to have been activated by blast vibrations, occurred in 1989 (Selamat, 1992). Incidents such as this prompted a funding at an Australian research institution for the necessary research to be carried out in which the author was involved (Selamat, 1992 and 1994).

When seeking for a convenient slope stability assessment procedure which incorporates the elements of a dynamic analysis as well as maintaining the simplicity of a static method, Sarma's method (Sarma, 1973, 1975, and 1979; and Sarma and Bhave, 1974) is the first thing to come to the minds of most engineers. Instead of the traditional FOS, Sarma suggests that the stability of a slope be evaluated based upon the amount of ground acceleration which can bring the slope to the threshold of failure. Later, Hoek modifies Sarma's method by incorporating FOS into the analysis (Hoek, 1987); thus FOS is now directly related to ground acceleration. If Sarma merely says that in a static problem, the traditional FOS model can be replaced by the new critical ground acceleration criterion, Hoek points out that the new procedure can be used to analyse a dynamic problem as well.

As the aim of this study is to verify the suitability of Sarma's method for analyzing the stability of slopes in a dynamic environment, the bases of the procedure are rederived, a minor rectification to Hoek's formulation (Hoek, 1987) is made, some significant aspects of FOS-acceleration curve are pointed out, and a case study on a slope using the procedure is reported.

BASIC FACTOR OF SAFETY (FOS) FORMULATIONS

In the following derivations, Eq. (1) to Eq. (3) represent the more traditional conceptions of FOS formulas. Eq. (4) is made up based on Sarma's procedure, except that here, as for the derivation of the three other equations, the failing body is a single block, while in the established Sarma's derivation, the implied number of slices are more than one. As shown in Fig. 1, based upon the principle of limit equilibrium, by applying the simple Mohr-Coulomb failure criterion, and by incorporating pre-tensioned bolt, T; horizontal ground acceleration, K_g; failing body weight, m_g; angle of friction, ϕ; and cohesion, c; the FOS expression is given by:

$$\text{FOS} = \frac{m_g \cos\alpha \, \tan\phi \, - \, m K_g \sin\alpha \, \tan\phi \, + \, T \sin(\alpha+\beta) \tan\phi \, + \, cb \sec\alpha}{m_g \sin\alpha \, + \, m K_g \cos\alpha \, - \, T \cos(\alpha+\beta)} \qquad (1)$$

The indication whether the bolt is pre-tensioned or not is reflected in the formula by either the bolt tension being that which reduces the failing load or that which adds to the resisting force. For the non-pre-tensioned bolt, the FOS is presented by:

$$\text{FOS} = \frac{m_g \cos\alpha \, \tan\phi \, - \, m K_g \sin\alpha \, \tan\phi \, + \, T \sin(\alpha+\beta) \tan\phi \, + \, T \cos(\alpha+\beta) \, + \, cb \sec\alpha}{m_g \sin\alpha \, + \, m K_g \cos\alpha} \qquad (2)$$

The derivation of Eq. (3) begins by noting that Eq. (1) and Eq. (2) give the same FOS value at limit equilibrium condition. When FOS equals unity in both equations, they are presented in an expression as:

$$\frac{m_g \cos\alpha \, \tan\phi \, - \, m K_{c_g} \sin\alpha \, \tan\phi \, + \, T \sin(\alpha+\beta) \tan\phi \, + \, cb \sec\alpha}{m_g \sin\alpha \, + \, m K_{c_g} \cos\alpha \, - \, T \cos(\alpha+\beta)}$$

$$= \frac{m_g \cos\alpha \, \tan\phi \, - \, m K_{c_g} \sin\alpha \, \tan\phi \, + \, T \sin(\alpha+\beta) \tan\phi \, + \, T \cos(\alpha+\beta) \, + \, cb \sec\alpha}{m_g \sin\alpha \, + \, m K_{c_g} \cos\alpha} \qquad (3)$$
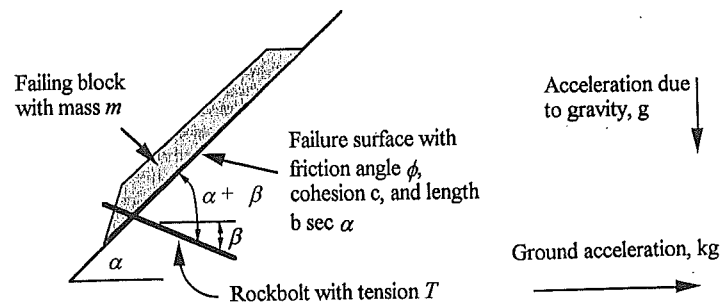

Fig. 1 A Single Block Failing Body

where K_{c_g} is the critical acceleration or acceleration at the threshold of failure. Solving the expression for K_c, and incorporating FOS for all strength parameters which are tan ϕ, T, and c, Eq. (3) can be presented as:

$$K = \frac{m_g[(\cos\alpha \, \tan\phi \, / \text{FOS}) - \sin\alpha] + (T/\text{FOS})\{[\sin(\alpha+\beta)\tan\phi \, / \text{FOS}] + \cos(\alpha+\beta)\} + (cb \sec\alpha)/\text{FOS}}{m_g[\cos\alpha \, + \, (\sin\alpha \, \tan\phi \, / \text{FOS})]} \qquad (4)$$

where, in case of Eq. (1) and Eq. (2), FOS is made to vary with changing ground acceleration. The difference is, in this instance, FOS at a certain ground acceleration level is not readily obtainable, as trial and error or computational process is required in getting the value.

In deriving Sarma's implied expression for a single block arrangement, basic multislice derivation technique is used whereby first, the equations for horizontal and vertical equilibriums are written. Next, the expressions for normal forces in horizontal and vertical equilibrium equations are solved. Since the normal forces for both expressions are the same entity, the horizontal and vertical equilibrium equations can be combined by eliminating these normal forces. The remaining notation can then be presented as (Selamat, 1995):

$$\frac{m_g \, + \, T\sin\beta \, - \, cb \sec\alpha \, \sin\alpha}{\cos\phi \, \cos\alpha \, + \, \sin\phi \, \sin\alpha} = \frac{K_c m_g \, - \, cb \sec\alpha \, \cos\alpha \, - \, T\cos\beta}{\sin\phi \, \cos\alpha \, - \, \cos\phi \, \sin\alpha} \qquad (5)$$

Solving for K_c, the final form is given by:

$$K_c = \frac{[(m_g + T\sin\beta)\sin(\phi-\alpha) \, + \, T\cos\beta \, \cos(\phi-\alpha) \, + \, (cb \cos\phi \, / \cos\alpha)]}{m_g \cos(\phi-\alpha)} \qquad (6)$$

and in obtaining FOS versus ground acceleration relationship, the FOS value is incorporated by substituting for the strength terms T, c, and $\tan\phi$ to become T/FOS, c/FOS, and $\tan\phi/\text{FOS}$, respectively in each round of computation. Critical acceleration, K_c becomes acceleration, K when FOS is incorporated into the expression.

Much can be said on the meaning and accuracy of these expressions but as this paper is not intended for such purpose, only a brief comment is offered here. Eq. (1) and Eq. (2) for example, do not imply that all strength parameters, i.e., tan ϕ, T, and c, have the same individual FOS as the average left hand side value of the equations. Without further dwelling, basically, these basic derivations are to show that Sarma's equation for a single block arrangement is presentable as much as other limit equilibrium expressions. In fact, one will find that Eq. (4) can be expanded and worked out to become Eq. (6).

SARMA'S METHOD

Sarma's original formulations are based upon a multislice failing body slope configuration (Fig. 2). As an analytical requirement, each slice must daylight at the slope surface and at the same time touches the failure surface. One of the many advantages of the method is that there is no restriction on slicing; that is, it can be horizontal, vertical, or in between. At these slice surfaces, Sarma's method also allows the calculations of normal and shear stresses. Obviously, normal forces must either be compressive or zero. An excessive negative value for these are unacceptable unless justified, for example, by the presence of cohesive material which sustains a very small amount of tensile stress.

Limiting equilibrium occurs when the ground accelerates at K_{c_g} - the critical acceleration. This is the acceleration when all sliding surfaces are assumed to be at the threshold of failure simultaneously, Sarma's original formulation evaluates static stability according to the value of K_c - the higher the K_c the more stable is the slope. Even without ground acceleration, a slope can be in the state of limit equilibrium, that is when K_c equals zero. The conventional limit equilibrium equivalence of this case is when FOS equals unity. Note that the original Sarma method alone does not give any static FOS; instead, K_c is the safety indicator.

While Sarma's method alone does not have any notion of FOS, Hoek's modified version does just that, that is to relate ground acceleration, K, to FOS (Hoek, 1987). The value of strength parameters T, c, and tan ϕ for all sliding
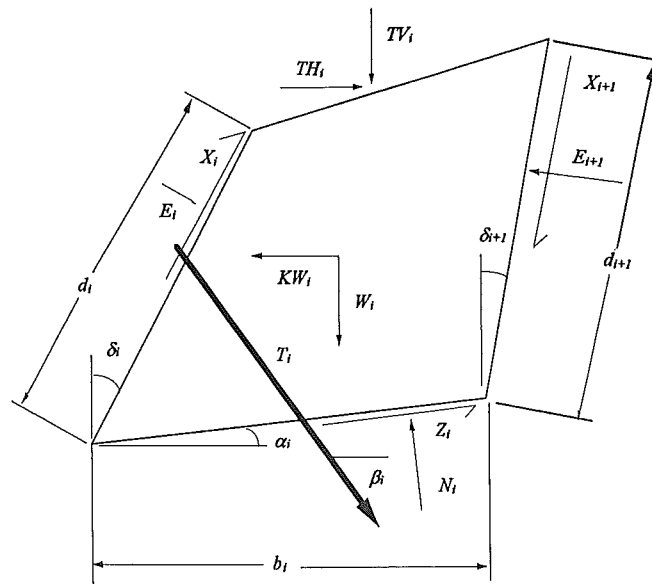
Fig. 2 Stability Analysis by Sarma's Method

surfaces are altered simultaneously by dividing them by the same FOS for each new K computation. Thus, a relationship between ground acceleration, K, and FOS is obtained. As FOS = 1, $K = K_C$.

Also, in this paper, the parameter of bolt tension is added in the analyses where its prestressed value is incorporated as an additional support for the first or the bottom most slice.

Sarma's formulation assumes the following:

1. Two dimensionality.
2. Rigid slice shapes, which means that the slices do not deform during load application nor during failure. Within each slice, there are no surfaces along which sub-failures occur.
3. Simultaneous failure, which means that the shear forces developed on all interslice and failure surfaces approach shear strengths simultaneously.
4. Mohr-Coulomb failure criterion.
5. Kinematic failure feasibility, which means that the failures are assumed feasible although geometrically not. Consider a rigid slice whose motion for failure is prevented by the nature of the geometry of a failure surface; in this case, once strengths are overcome, slices are assumed failing.
6. Equal FOSs for all strength parameters. FOSs are simultaneously based on three strength parameters which are $\tan\phi$, T, and c. Thus all should be assigned with design values.

A unified formulation for Sarma's method is shown in Fig. 2 where:

E_i and E_{i+1}	=	Total normal force exerted onto slice i sides by neighboring slices and water;
X_i and X_{i+1}	=	Total shear force exerted onto slice i sides by neighboring slices;
N_i	=	Total normal force exerted onto slice base;
Z_i	=	Total shear force exerted onto slice base;
W_i and KW_i	=	Slice weight and induced horizontal force due to ground acceleration. W_i equals $m_i\,g$ where m_i is mass of slice i and g is acceleration due to gravity;

TV_i and TH_i	=	Total vertical and horizontal external forces exerted on the slice. These forces are not incorporated in the calculation of critical acceleration in the original Sarma method but appears in the Hoek's formulation (Hoek, 1987);
T_i	=	Mobilized rock bolt tension. This force is introduced in the current derivation;
b_i and d_i	=	Horizontal length of base i and actual length of side i;
c_{si}, $\tan\phi_{si}$	=	Cohesion and angle of friction of base i;
c_{si}, $\tan\phi_{si}$	=	Shear strength values of side i;
U_i, PW_i	=	Pore water forces for base i, side i;
and PW_{i+1}	=	and for side $i+1$;
δ_i and δ_{i+1}	=	Angle between vertical and side i and angle between vertical and side $i+1$.

A unified derivation of Sarma's method incorporating external forces and rockbolts is given in Appendix A. The minor rectification to Hoek's formulation (Hoek 1987) is also pointed out therein. The results are presented as a relationship between FOS and ground acceleration expressed by K_g.

AN IMPORTANT IMPLICATION OF FOS-ACCELERATION RELATIONSHIP

When considering the dynamic stability of a slope, to one's first impression, a slope with a higher static FOS would also have a higher K_c, as one would immediately think that such a slope would require a higher ground acceleration to bring it to the threshold of failure. But according to the general shape of FOS-acceleration relationships as shown in Fig. 3, this is not constantly true. Although a result of Sarma's analysis always gives the characteristic curve, its relative positioning tells of different possibilities in safety assessment.

In Fig. 3, for Curve I, the zero acceleration axis lies at the steeper portion of the relationship. Curve II is relatively shifted to the left, and slightly raised, moving its steep portion away from zero acceleration. Obviously, although Curve I shows a high static FOS, it does not take as much ground acceleration to bring the structure to the threshold of failure. In Curve II, although the static FOS is low, the slope is in fact safer under a similar ground acceleration intensity, because failure occurs at a much higher acceleration than with Curve I. This is a paradox, that evaluating slope safety according to only one criterion is insufficient; conventional static FOS and critical acceleration, K_c are both indicators of slope stability and the need to present them together in any assessment is proposed. A slope will not be free from the effects of one form of ground acceleration or another throughout it's lifetime.

CASE STUDY

Generally, the critical factors which affect static FOS include soil parameters, slope geometry, and ground water conditions. But to analyze the effects of ground acceleration, additional information on vibration record is necessary. In this section, an actual slope stability case in a mining environment is studied whereby the extended Sarma method is employed using soil parameters, slope geometry, and ground acceleration levels of the site. Reflecting the actual dry condition at the diamond mine site in Botswana, there is no ground water consideration to be included in the analysis. In this simplified manner, the applicability of the procedure is even better presented.

The geology of this location consists of an upper layer of dry calcrete, 20 m thick, which lies on top of Transvaal Shale that extends to the toe of the slope and beyond (Fig. 4). The deposit at the site is rubbly and has no discernible structures except for occasional termite burrow remnants. The underlying shale - joint surveyed - is heavily jointed with between 4 to 24 fractures per meter, with the discontinuities being weathered and incompetent, to being pronounced and visible, to being masked and nonexistent. The stereographic projection plot indicates that these joints are prominently dipping in the direction of the cut but are gentle enough that a modest shear strength would hold them against sliding. The Rock Mass Rating for the shale is 42. Tests on cores classify the shale as medium strong with compressive strength varying between 50 MPa and 270 MPa and that the specimens can be fractured with single firm geological hammer blow but cannot be peeled or scraped by a knife. Unit mass varies between 2670 kg/m^3 to 3030 kg/m^3.

It is at the shale layer where joints would play the dominant role in determining the failure surface. The concern for slope stability at this location is due to some joint dips which plot in the kinematic instability region of the stereographic projection. There was no major failure in the past, but as the size of the slope involved is increasing, and so are the blastings, which at times are very near, the concern against falling is well founded, statically and

Fig. 3   Relative Positioning of Sarma's FOS-Accelerated Curve

Fig. 4   Botswanan Slope Case Study

Jwaneng section A, Slicing type 1, JWA1
No. of slices: 7
No. of sides: 8
Coordinates:

Side	Top	Coordinate (x,y)	Bottom	Coordinate(x,y)	c	Ø
1	0.0000	0.0000	0.0000	0.0000	0	0
2	23.0000	24.0000	29.0000	14.0000	0	34
3	32.0000	26.0000	37.0000	18.0000	0	34
4	38.0000	35.0000	46.0000	22.0000	0	34
5	44.0000	36.0000	51.0000	25.0000	0	35
6	62.0000	57.0000	75.0000	36.0000	0	35
7	72.0000	50.0000	81.0000	39.0000	0	35
8	85.0000	50.0000	85.0000	50.0000	0	0

Slice	Mass (kg)	Base c	Base Ø
1:	514250	0	34
2:	255750	0	34
3:	332750	0	34
4:	222750	0	34
5:	0.131936E+07	0	35
6:	281960	0	35
7:	190190	0	35

Total mass: 0.311701E + 07 kg.

Jwaneng Section A, Slicing type 3, JWA3
No. of slices: 10
No. of sides: 11
Coordinates:

Side	Top	Coordinate (x,y)	Bottom	Coordinate(x,y)	c	Ø
1	0.0000	0.0000	0.0000	0.0000	0	0
2	23.0000	24.0000	23.0000	11.0000	0	34
3	33.0000	26.0000	33.0000	16.0000	0	34
4	39.0000	35.0000	39.0000	19.0000	0	34
5	44.0000	36.0000	44.0000	22.0000	0	35
6	60.0000	55.0000	60.0000	31.0000	0	35
7	63.0000	56.0000	63.0000	33.0000	0	35
8	72.0000	50.0000	72.0000	36.0000	0	35
9	80.0000	50.0000	80.0000	40.0000	0	35
10	83.0000	50.0000	83.0000	44.0000	0	35
11	85.0000	50.0000	85.0000	50.0000	0	35

Slice	Mass (kg)	Base c	Base Ø
1:	411125	0	34
2:	316250	0	34
3:	214500	0	34
4:	206250	0	34
5:	808640	0	35
6:	187530	0	35
7:	442890	0	35
8:	255360	0	35
9:	63840.0	0	35
10:	15960.0	0	35

Total mass: 0.292235E + 07 kg

Jwaneng section A, Slicing type 2, JWA2
No. of slices: 8
No. of sides: 9
Coordinates:

Side	Top	Coordinate (x,y)	Bottom	Coordinate(x,y)	c	Ø
1	0.0000	0.0000	0.0000	0.0000	0	0
2	21.0000	20.0000	40.0000	20.0000	0	34
3	24.0000	24.0000	48.0000	24.0000	0	34
4	32.0000	26.0000	52.0000	26.0000	0	34
5	38.0000	35.0000	72.0000	35.0000	0	35
6	44.0000	36.0000	74.0000	36.0000	0	35
7	63.0000	56.0000	76.0000	37.0000	0	35
8	72.0000	50.0000	82.0000	41.0000	0	35
9	85.0000	50.0000	85.0000	50.0000	0	0

Slice	Mass (kg)	Base c	Base Ø
1:	522500	0	34
2:	236500	0	34
3:	121000	0	34
4:	668250	0	34
5:	85120.0	0	35
6:	865830	0	35
7:	248710	0	35
8:	155610	0	35

Total mass: 0.290352E + 07 kg.

Jwaneng section A, Slicing type 4, JWA4
No. of slices: 8
No. of sides: 9
Coordinates:

Side	Top	Coordinate (x,y)	Bottom	Coordinate(x,y)	c	Ø
1	0.0000	0.0000	0.0000	0.0000	0	0
2	23.0000	24.0000	48.0000	24.0000	0	34
3	33.0000	26.0000	52.0000	26.0000	0	34
4	38.0000	35.0000	55.0000	28.0000	0	35
5	44.0000	36.0000	69.0000	34.0000	0	35
6	62.0000	57.0000	69.0000	34.0000	0	35
7	72.0000	50.0000	72.0000	35.0000	0	35
8	82.0000	50.0000	82.0000	42.0000	0	35
9	85.0000	50.0000	85.0000	50.0000	0	0

Slice	Mass (kg)	Base c	Base Ø
1:	825000	0	34
2:	121000	0	34
3:	310750	0	34
4:	315210	0	35
5:	746130	0	35
6:	300580	0	35
7:	305900	0	35
8:	31920.0	0	35

Total mass: 0.295649E + 07 kg

Fig. 5   Slicing Input of Botswanan Slope Case Study for a Sarma Type Analysis

dynamically. As depicted in Fig. 4, the dominant joint dippings critical for sliding lie 30° to 55° below horizontal. This observation, together with closer site inspections, provid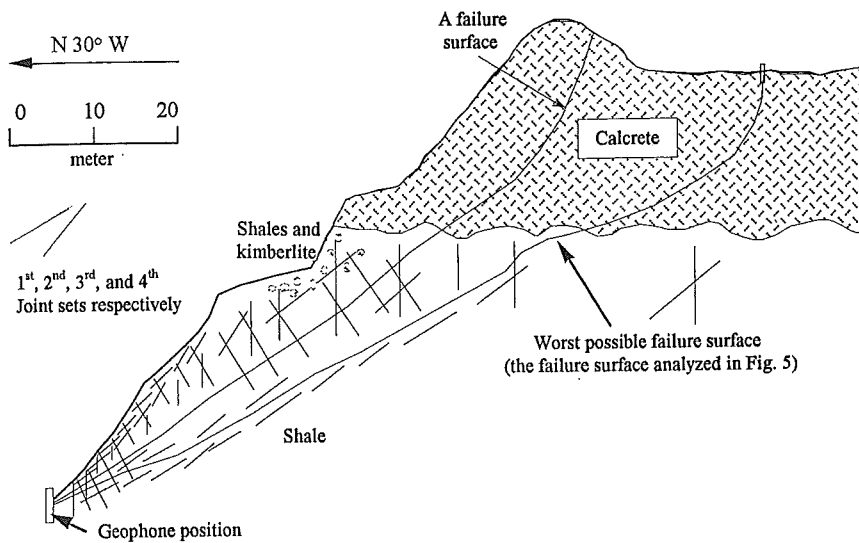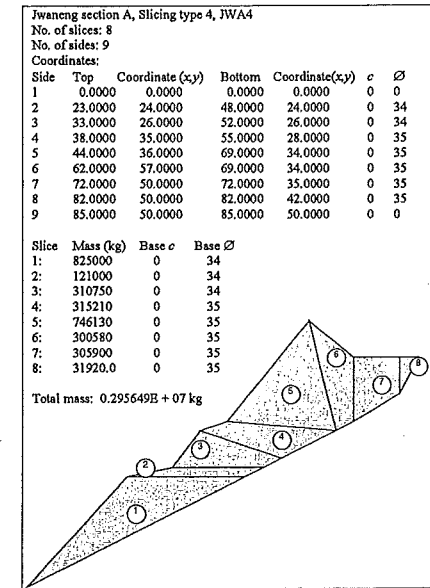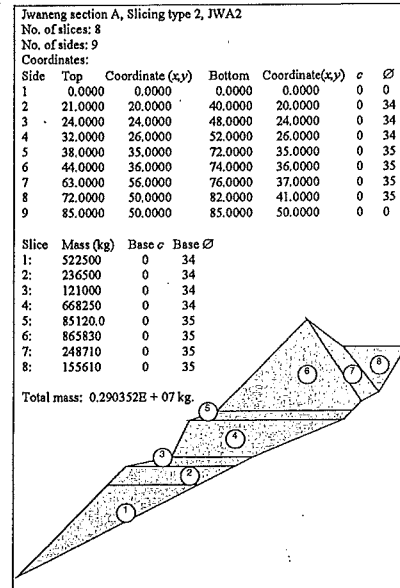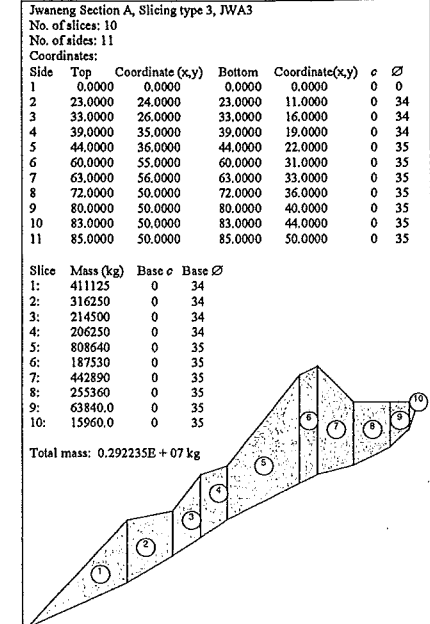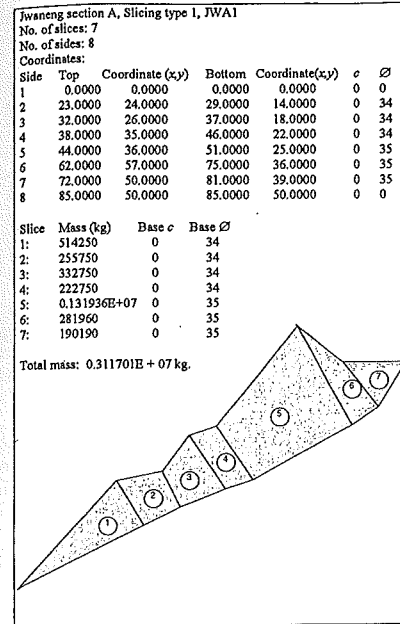e the bases for failure surface appointment within the shale region; for overlying calcrete, the failure delineation is a hand drawn approximate.

The angle of friction for shale samples ranges between 13.7° and 66.2° and cohesions are almost zero. For calcrete, the angle of friction extends between 31.7° and 32.0° while cohesions are about 6.8 MPa. But for this analysis, friction angles of 34° and 35° are used for shale and calcrete respectively while cohesions for all are assumed nil. Unit masses for the two materials are taken as 2750 kg/m³ and 2660 kg/m³.

Generally accepted, the slicing in Sarma's method should be in accordance with the actual delineation, as observed during the joint survey. Nevertheless, in this work, the slicing sensitivity is examined by altering inputs on node positions (Fig. 5). The result of Sarma's analysis indicates that FOS difference is relatively small for a good range of acceleration (Fig. 6), especially in the vicinity of FOS equals unity.

For every Sarma's analysis, acceptability of the solution must be verified. This specifically means that base and interslice stresses must not be significantly negative, a condition otherwise impossible to interpret, and reappointing nodal positions becomes necessary. This paper nevertheless presents a rectified analysis where base and interslice normal stresses within a certain FOS range are free of excessive negative values and the solution is therefore acceptable (Table 1).

From Fig. 6, for all slicing types, the static FOS lies in the range of 1.3 to 1.4, an acceptable level in the mining practice. The critical acceleration, K_{cg}, is about 2 m/s², meaning that the slope would stand a ground acceleration intensity up to that level, a uniform one along the slope such as that which comes from an earthquake, and long enough for the failure mechanisms to take full effect.
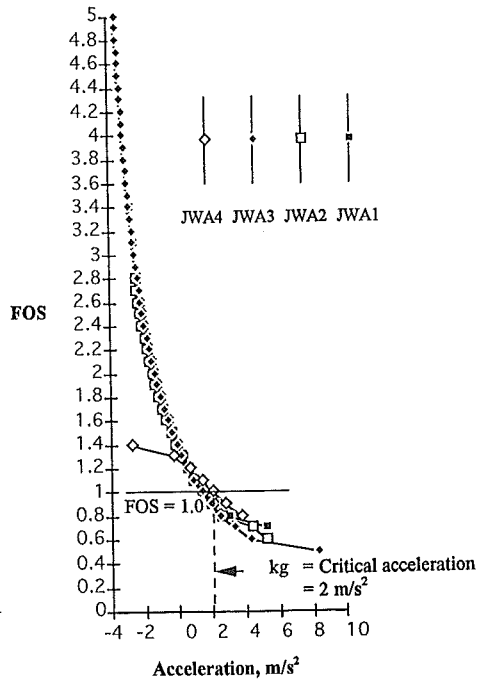
FOS

y-axis (FOS): 5, 4.8, 4.6, 4.4, 4.2, 4, 3.8, 3.6, 3.4, 3.2, 3, 2.8, 2.6, 2.4, 2.2, 2, 1.8, 1.6, 1.4, 1.2, 1, 0.8, 0.6, 0.4, 0.2, 0

x-axis (Acceleration, m/s²): -4, -2, 0, 2, 4, 6, 8, 10

JWA4   JWA3   JWA2   JWA1

FOS = 1.0

kg = Critical acceleration = 2 m/s²

Fig. 6 Result of Sarma Type Analysis on Botswanan Slope Case Study

Table 1 Base and Interslice Stresses by Sarma's Method on Botswanan Slope Case Study

JWA1 Interslice Stresses

FOS	Side 1 (Pa)	Side 2 (Pa)	Side 3 (Pa)	Side 4 (Pa)	Side 5 (Pa)	Side 6 (Pa)	Side 7 (Pa)	Side 8 (Pa)
1.4	0.000000	435.692	222.517	2532.48	-256.068	3820.78	8836.61	0.000000
1.3	0.000000	256.157	-167.001	1313.03	-746.617	3745.53	8962.04	0.000000
1.2	0.000000	-4.67419	-737.598	994.937	-1461.23	3639.15	9156.66	0.000000
1.1	0.000000	-426.870	-1667.84	475.472	-2615.35	3457.75	9455.69	0.000000
1.0	0.000000	-1234.95	-3461.61	-543.410	-4808.09	3064.52	9920.43	0.000000

JWA2 Interslice Stresses

FOS	Side 1 (Pa)	Side 2 (Pa)	Side 3 (Pa)	Side 4 (Pa)	Side 5 (Pa)	Side 6 (Pa)	Side 7 (Pa)	Side 8 (Pa)	Side 9 (Pa)
1.2	0.000000	-112.566	-129.451	-180.106	-1334.45	-1595.73	4797.78	8683.74	0.000000
1.1	0.000000	46.5777	53.5644	74.5243	-954.070	-1142.66	4801.27	9088.18	0.000000
1.0	0.000000	200.053	230.061	320.085	-595.387	-714.968	4733.58	9698.98	0.000000
0.9	0.000000	352.687	405.590	564.300	-249.357	-302.357	4328.57	10663.3	0.000000
0.8	0.000000	465.814	535.686	745.303	22.1845	22.7993	1654.30	12279.9	0.000000
0.7	0.000000	2653.26	3051.25	4245.21	5575.79	4278.89	56343.1	17216.4	0.000000
0.6	0.000000	2361.74	2716.00	3778.78	2716.00	3817.68	25509.5	25808.3	0.000000
0.5	0.000000	14325.7	16474.5	22921.1	22317.3	26728.8	118600.	144947.	0.000000

JWA3 Interslice Stresses

FOS	Side 1 (Pa)	Side 2 (Pa)	Side 3 (Pa)	Side 4 (Pa)	Side 5 (Pa)	Side 6 (Pa)	Side 7 (Pa)	Side 8 (Pa)	Side 9 (Pa)	Side 10 (Pa)	Side 11 (Pa)
2.0	0.000000	799.554	1313.12	936.726	143.376	-830.228	-1674.01	2455.22	3954.32	2096.65	0.000000
1.9	0.000000	776.676	1260.80	894.454	88.5461	-869.104	-1712.80	2405.61	3877.62	2038.02	0.000000
1.8	0.000000	752.866	1205.75	849.830	29.5013	-912.318	-1756.94	2355.84	3800.60	1978.83	0.000000
1.7	0.000000	728.533	1147.69	802.533	-34.5693	-960.954	-1807.88	2306.32	3723.77	1919.27	0.000000
1.6	0.000000	702.194	1085.98	752.127	-104.777	-1016.51	-1867.60	2257.56	3647.89	1859.63	0.000000
1.5	0.000000	675.149	1020.17	698.002	-182.683	-1081.14	-1938.95	2210.35	3573.95	1800.26	0.000000
1.4	0.000000	646.756	949.234	639.245	-270.571	-1157.95	-2026.05	2165.74	3503.37	1741.64	0.000000
1.3	0.000000	616.718	871.659	574.430	-371.923	-1251.74	-2135.19	2125.34	3438.16	1684.43	0.000000
1.2	0.000000	584.461	784.852	501.153	-492.350	-1370.14	-2276.31	2091.55	3381.21	1629.56	0.000000
1.1	0.000000	548.798	684.047	415.070	-641.481	-1526.02	-2466.06	2068.17	3336.83	1578.33	0.000000
0.9	0.000000	507.036	559.616	307.568	-837.262	-1742.90	-2734.40	2061.63	3311.67	1532.63	0.000000

JWA4 Interslice Stresses

FOS	Side 1 (Pa)	Side 2 (Pa)	Side 3 (Pa)	Side 4 (Pa)	Side 5 (Pa)	Side 6 (Pa)	Side 7 (Pa)	Side 8 (Pa)	Side 9 (Pa)
1.5	0.000000	7424.5	112014.	-377946	-305597.1	306744.4	2320.54	5171.38	0.000000
1.4	0.000000	-18502.4	-279915.9	164735.	280082.2	-5403.19	-1676.51	1751.21	0.000000
1.3	0.000000	-2751.61	-4136.46	67580.4	166909.4	1424.37	2873.25	2285.62	0.000000
1.2	0.000000	932.981	1407.66	42409.1	136712.9	3575.73	4168.29	2382.36	0.000000
1.1	0.000000	2406.36	3630.66	30924.5	110922.3	5049.98	4917.34	2405.37	0.000000
1.0	0.000000	3166.16	4777.01	24554.3	110922.7	6636.14	5573.52	2440.09	0.000000
0.9	0.000000	3720.06	5612.72	20946.3	10749.5	9071.55	6382.36	2530.34	0.000000
0.8	0.000000	4537.85	6846.58	19949.9	11526.8	14661.4	7812.94	2530.34	0.000000
0.7	0.000000	9401.68	14185.0	321473.	21334.4	51510.4	14356.1	3134.60	0.000000

JWA1 Base Stresses

FOS	Base 1 (Pa)	Base 2 (Pa)	Base 3 (Pa)	Base 4 (Pa)	Base 5 (Pa)	Base 6 (Pa)	Base 7 (Pa)
1.6	14449.0	25461.1	31851.8	31188.8	48661.1	43077.7	7291.92
1.5	14262.3	25083.3	31576.1	30437.2	48278.6	42870.7	7268.53
1.4	14047.6	24643.2	31275.1	29540.6	47874.0	42706.4	6530.89
1.3	13795.7	24116.7	30945.8	28437.1	47454.5	42630.9	5687.00
1.2	13490.0	23460.3	30590.6	27014.0	47039.3	42739.4	4704.76
1.1	13096.9	22581.4	30208.9	25037.5	46679.2	43252.2	3534.68
1.0	12529.7	21231.2	29811.4	21909.6	46525.1	44782.3	2094.1
0.9	11453.7	18392.4	24410.7	15408.0	47208.4	49754.1	225.222

JWA2 Base Stresses

FOS	Base 1 (Pa)	Base 2 (Pa)	Base 3 (Pa)	Base 4 (Pa)	Base 5 (Pa)	Base 6 (Pa)	Base 7 (Pa)	Base 8 (Pa)
1.4	10000.1	22631.9	23158.2	24100.2	32451.8	420890.	32563.3	4862.63
1.3	9925.12	22462.1	22984.5	24160.3	32266.4	409524.	32185.2	3923.71
1.2	9821.30	22272.2	22744.1	24127.7	31979.5	398406.	31870.8	2810.33
1.1	9687.11	21923.5	22433.3	24000.1	31586.2	387102.	31733.0	1452.90
1.0	9519.53	21544.2	22045.2	23771.4	31076.9	374716.	32080.4	-266.770
0.9	9312.78	21076.3	21566.4	23428.6	30432.9	358234.	33996.3	-2566.30
0.8	9043.72	20467.4	20943.4	22916.6	29579.8	317742.	44189.0	-5874.69
0.7	9377.37	21222.5	21716.0	23822.8	30633.6	846843.	-127726	-14290.8

JWA3 Base Stresses

FOS	Base 1 (Pa)	Base 2 (Pa)	Base 3 (Pa)	Base 4 (Pa)	Base 5 (Pa)	Base 6 (Pa)	Base 7 (Pa)	Base 8 (Pa)
1.4	14195.2	24693.7	27914.6	28893.9	38857.7	8503.9	45842.9	25771.8
1.3	13997.4	24317.6	27489.5	29272.5	38146.5	77359.4	45721.9	25394.5
1.2	13773.1	23889.9	27006.0	28561.6	37337.2	62929.2	45629.0	24968.0
1.1	13516.3	23398.2	26450.2	27737.3	36405.0	99930.8	45595.9	24481.4
1.0	13219.0	22825.0	25802.2	26763.4	35313.6	880812.	45686.3	23919.9
0.9	12869.0	22143.5	25031.8	25581.1	34005.1	0.180E+07	46038.6	23261.4
0.8	12445.4	21305.9	24084.9	24081.0	32373.7	34835.3	46993.7	22467.2
0.7	11898.6	20199.4	22834.1	22005.6	30171.6	31490.7	49595.6	21443.7
0.6	10996.1	18349.4	20742.8	18392.2	26450.0	26061.7	58865.4	19738.4

JWA4 Base Stresses

FOS	Base 1 (Pa)	Base 2 (Pa)	Base 3 (Pa)	Base 4 (Pa)	Base 5 (Pa)	Base 6 (Pa)	Base 7 (Pa)	Base 8 (Pa)
1.4	13357.0	23508.3	283210.	-12658.5	495536.	8503.9	19919.5	2714.83
1.3	13683.1	24082.3	211791.	-1811.53	575033.	77359.4	18761.7	2433.05
1.2	13665.3	24051.0	171899.	3861.70	643829.	62929.2	17508.8	2140.39
1.1	13502.7	23764.8	147614.	6991.28	726155.	99930.8	15966.8	1816.02
1.0	13357.4	23509.0	134835.	8424.23	880812.	-13396.8	13707.7	1421.78
0.9	14524.1	25562.5	162207.	5981.96	0.180E+07	-370104.	6799.03	622.974

Note: FOSs free of excessive negative stresses (>2000 Pa) area highlighted in bold
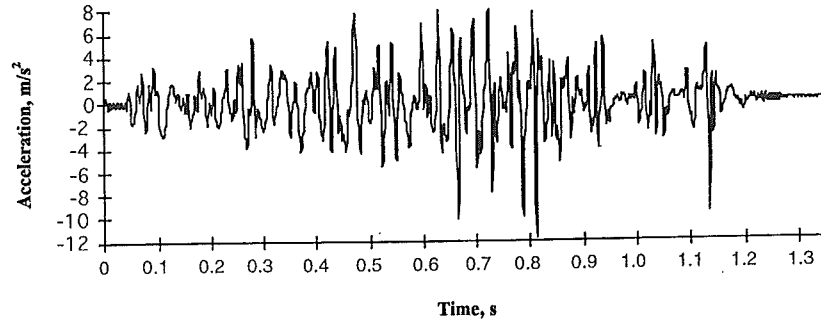
Fig. 7 Recorded Blast Signal from Botswanan Slope Case Study

For a stability analysis during ground vibration period, values from an associated ground acceleration waveform are used. Figure 7 is a blast acceleration waveform of the site. Simply stated, the maximum horizontal acceleration of about 8 m/s² or more implies a FOS value of less than unity. Pseudo-statically, one may interpret that there are instances - albeit each happens only for a fraction of a second - where the slope is in a state of failure. But for this high frequency blast vibrations, only a portion of the slope is effected by a particular high acceleration at any particular instance. Should the concern is a low frequency earthquake acceleration waveform, where a larger portion of the slope is subjected to the same acceleration at the same time, each occurrence of high acceleration would probably fail the slope.

These facts, which consider that acceleration varies along the slope length, have lead to the development of a new concept of net acceleration. Net acceleration addresses the fact that when the base of a structure is not subjected to the same prescribed motion, there is a realistic net acceleration that can be used to correlate with an FOS in Sarma's method. This however goes beyond the present Sarma's concept of a uniform, constant ground acceleration.

CONCLUSION

In this study, the latest version of Sarma's method by Hoek (1987) has been rederived and a minor but necessary rectification has been made. The implication of Sarma's curve in occupying a relative position in the FOS versus ground acceleration presentation has been noted and described. Thus, static FOS and critical acceleration, K_c, are both important indication for presenting safety assessment for most of today's slopes, which, not only that its static FOS be acceptable, but also, in its lifetime, would be subjected to one form or another of accelerating ground, which then requires an acceptable dynamic safety indicator. The case study presents an example where the slope responds to ground acceleration according to the current Sarma's method. A new concept of describing net acceleration is necessary in addressing the fact that ground acceleration of a high frequency source, such as a production blast, or a traffic pass, is not uniform along a slope; this however, is not within the scope of current discussion.

ACKNOWLEDGMENT

REFERENCES

HOEK, E. (1987). General two-dimensional slope stability analysis. *Analytical and Computational Method in Engineering Rock Mechanics*, pp. 95-128.

SARMA, S.K. (1973). Stability analysis of embankments and slope. *Geotechnique*, No. 23, pp. 423-433.

SARMA, S.K. (1975). Seismic stability of earth dams and embankments. *Geotechnique*, No. 25, pp. 43-76.

SARMA, S.K. (1979). Stability analysis of embankments and slopes. *Journal of the Geotechnical Engineering Division, ASCE*, No. 105, GT12, pp. 1511-1524.

SARMA, S.K., and BHAVE, M.V. (1974). Critical acceleration versus static Factor of Safety in stability analysis of earth dams and embankments. *Geotechnique*, No. 24, pp. 661-665.

SELAMAT, M.R. (1992). A two dimensional rock slope stability analysis incorporating blast vibrations. *Proceedings of the JKMRC Conference*, Brisbane, Australia.

SELAMAT, M.R. (1995). Rock Slope Stability Incorporating Blast Vibrations. Ph.D. Thesis, Julius Kruttschnitt Mineral Research Centre, University of Queensland, Australia.

SELAMAT, M.R. (1996). Blasting practices and the stability of slopes at cuttings, quarries, and natural rock faces in Perak. *Proceedings of the 12th Southeast Asian Geotechnical Conference (12SEAGC)*, Kuala Lumpur, Malaysia. pp. 479-485.

SELAMAT, M.R., and MOHAMMAD, M.A. (1996). Stability aspects of limestone cliffs and cuts associated with production and cut blastings. *Proceedings of the International Symposium on Limestone (LIMESTONE 96)*, Kuala Lumpur, Malaysia. pp. 160-165.

APPENDIX A

The following derivation of Sarma's Method is based on the parameters described in the text. Considering limit equilibrium condition, for slice i:

$$N_i\cos\alpha_i + Z_i\sin\alpha_i = W_i + X_{i+1}\cos\delta_{i+1} - X_i\cos\delta_i - E_{i+1}\sin\delta_{i+1} + E_i\sin\delta_i + TV_i + T_i\sin\beta_i \quad (7)$$

and

$$Z_i\cos\alpha_i - N_i\sin\alpha_i = K_cW_i + X_{i+1}\sin\delta_{i+1} - X_i\sin\delta_i + E_{i+1}\cos\delta_{i+1} - E_i\cos\delta_i - TH_i - T_i\cos\beta_i \quad (8)$$

By assuming Mohr-Coulomb failure criterion for bases and sides shear strength:

$$Z_i = (N_i - U_i)\tan\phi_{Bi} + c_{Bi}\,b_i\sec\alpha_i \quad (9)$$

$$X_i = (E_i - PW_i)\tan\phi_{Si} + c_{Si}d_i \quad (10)$$

$$X_{i+1} = (E_{i+1} - PW_{i+1})\tan\phi_{Si+1} + c_{Si+1}d_{i+1} \quad (11)$$

By substituting Eq. (9), Eq. (10), and Eq. (11) into Eq. (7) and Eq. (6) and solving:

$$(E_{i+1})\,\frac{\cos(\phi_{Bi}-\alpha_i+\phi_{Si+1}-\delta_{i+1})\sec(\phi_{Si+1})}{\sin(\phi_{Bi}-\alpha_i)\cos(\phi_{Bi}-\alpha_i)}$$

$$= \frac{1}{\cos(\phi_{Bi}-\alpha_i)}[W_i + TV_i + T_i\sin\beta_i] - \frac{1}{\sin(\phi_{Bi}-\alpha_i)}[K_cW_i - TH_i - T_i\cos\beta_i]$$

$$+ [c_{Si+1}d_{i+1}][\frac{\sin(\phi_{Bi}-\alpha_i-\delta_{i+1})}{\sin(\phi_{Bi}-\alpha_i)\cos(\phi_{Bi}-\alpha_i)}]$$

$$- \quad [PW_{i+1} \tan\phi_{Si+1}] \left[\frac{\sin(\phi_{Bi} - \alpha_i - \delta_{i+1})}{\sin(\phi_{Bi} - \alpha_i)\cos(\phi_{Bi} - \alpha_i)} \right]$$

$$- \quad [c_{Si}\, d_i] \left[\frac{\sin(\phi_{Bi} - \alpha_i - \delta_i)}{\sin(\phi_{Bi} - \alpha_i)\cos(\phi_{Bi} - \alpha_i)} \right]$$

$$+ \quad [PW_i \tan\phi_{Si}] \left[\frac{\sin(\phi_{Bi} - \alpha_i - \delta_i)}{\sin(\phi_{Bi} - \alpha_i)\cos(\phi_{Bi} - \alpha_i)} \right]$$

$$+ \quad [c_{Bi}\, b_i] \left[\frac{\cos\phi_{Bi}}{\sin(\phi_{Bi} - \alpha_i)\cos(\phi_{Bi} - \alpha_i)\cos\alpha_i} \right]$$

$$- \quad [U_i \tan\phi_{Bi}] \left[\frac{\cos\phi_{Bi}}{\sin(\phi_{Bi} - \alpha_i)\cos(\phi_{Bi} - \alpha_i)} \right]$$

$$+ \quad [E_i] \left[\frac{\cos(\phi_{Si} - \alpha_i + \phi_{Bi} - \delta_i)}{\sin(\phi_{Bi} - \alpha_i)\cos(\phi_{Bi} - \alpha_i)\cos\phi_{Si}} \right] \tag{12}$$

Let: $\qquad Q_i \quad = \quad \dfrac{1}{\cos(\phi_i - \alpha_i + \phi_{Si+1} - \delta_{i+1})\sec(\phi_{Si+1})} \tag{13}$

knowing: $\qquad S_i \quad = \quad c_{Si}\, d_i - PW_i \tan\phi_{Si} \tag{14}$

$\qquad\qquad S_{i+1} \quad = \quad c_{Si+1}\, d_{i+1} - PW_{i+1} \tan\phi_{Si} \tag{15}$

$\qquad\qquad R_i \quad = \quad (c_{Bi}\, b_i)/(\cos\alpha_i) - U_i \tan\phi_{Bi} \tag{16}$

and allowing: $\quad a_i \quad = \quad Q_i\{(W_i + TV_i + T_i\sin\beta_i)\sin(\phi_{Bi} - \alpha_i)$
$\qquad\qquad\qquad\qquad + (TH_i + T_i\cos\beta_i)\cos(\phi_{Bi} - \alpha_i) + S_{i+1}\sin(\phi_{Bi} - \alpha_i - \delta_{i+1})$
$\qquad\qquad\qquad\qquad - S_i\sin(\phi_{Bi} - \alpha_i - \delta_i) + R_i\cos\phi_{Bi}\} \tag{17}$

while letting: $\quad p_i \quad = \quad Q_i\, W_i \cos(\phi_{Bi} - \alpha_i) \tag{18}$

$\qquad\qquad e_i \quad = \quad [Q_i] \dfrac{\cos(\phi_{Si} - \alpha_i + \phi_{Bi} - \delta_i)}{\cos\phi_{Si}} \tag{19}$

Rewriting Eq. (12): $\; E_{i+1} \quad = \quad a_i - p_i K_c + E_i e_i \tag{20}$

which is a recurrence relation, for example:

$$E_2 \quad = \quad a_1 - p_1 K_c + E_1 e_1 \tag{21}$$

$$E_3 \quad = \quad a_2 - p_2 K_c + E_2 e_2 = a_2 + a_1 e_2 - p_2 K_c - p_1 e_2 K_c + E_1\, e_2 e_1 \tag{22}$$

$$E_4 \quad = \quad a_3 + a_2 e_3 + a_1 e_3 e_2 - p_3 K_c - p_2 e_3 K_c - p_1 e_3 e_2 K_c + E_1 e_3 e_2 e_1 \tag{23}$$

By proceeding to nth term:

$$E_{n+1} \quad = \quad (a_n + a_{n-1}e_n + a_{n-2}\,e_n e_{n-1} + \ldots \text{ to } n \text{ terms})$$
$$- K_c(p_n + p_{n-1}e_n - p_{n-2}e_n\,e_{n-1} + \ldots \text{ to } n \text{ terms})$$
$$+ E_1(e_n e_{n-1}e_{n-2}\ldots e_1) \tag{24}$$

$E_{n+1} = E_1 = 0$, since the external forces, TH_i, TV_i, $T\cos\beta$, and $T\sin\beta$ have been incorporated into the leading equations.

Therefore, by solving Eq. (24):

$$K_c \quad = \quad \frac{a_n + a_{n-1}\,e_n + a_{n-2}\,e_n e_{n-1} + \ldots + a_1\,e_n e_{n-1}\ldots e_3\,e_2}{p_n + p_{n-1}\,e_n + p_{n-2}\,e_n e_{n-1} + \ldots + p_1\,e_n e_{n-1}\ldots e_3\,e_2} \tag{25}$$

The slight error in Hoek's formulations is the negative sign in his relationship which corresponds to Eq. (17) (Hoek, 1987) where:

$$a_i \quad = \quad Q_i\{(W_i + TV_i)\sin(\phi_{Bi} - \alpha_i) - TH_i\cos(\phi_{Bi} - \alpha_i)$$
$$+ R_i\cos\phi_{Bi} + S_{i+1}\sin(\phi_{Bi} - \alpha_i - \delta_{i+1}) - S_i\sin(\phi_{Bi} - \alpha_i - \delta_i)\} \tag{26}$$

whereas it should have been a positive as in the current:

$$a_i \quad = \quad Q_i\{(W_i + TV_i + T_i\sin\beta_i)\sin(\phi_{Bi} - \alpha_i)$$
$$+ (TH_i + T_i\cos\beta_i)\cos(\phi_{Bi} - \alpha_i)$$
$$+ R_i\cos\phi_{Bi} + S_{i+1}\sin(\phi_{Bi} - \alpha_i - \delta_{i+1}) - S_i\sin(\phi_{Bi} - \alpha_i - \delta_i)\} \tag{27}$$

K versus FOS relationship is obtained by doing the following substitutions:

K for K_c, $\quad$ (T_i/FOS) for T_i, $\quad$ ($\tan\phi_{Bi}$/FOS) for $\tan\phi_{Bi}$, $\quad$ (c_{Bi}/FOS) for c_{Bi}, $\quad$ ($\tan\phi_{Si}$/FOS) for $\tan\phi_{Si}$,

(c_{Si}/FOS) for c_{Si}, $\quad$ (c_{Si+1}/FOS) for c_{Si+1}, $\quad$ and $\quad$ ($\tan\phi_{Si+1}$/FOS) for $\tan\phi_{Si+1}$